

On the Reaction of $[(\text{CO})_3\text{Fe}(\mu\text{-Me}_2\text{NCO})_2\text{Fe}(\text{CO})_2(\text{NHMe}_2)]$ with Chelating Ligands – X-Ray Structures of New Binuclear μ -Carbamoyl Complexes

Wolfgang Petz*, Bernhard Neumüller*, and Jens Pudewills

Marburg, Fachbereich Chemie der Philipps-Universität

Received February 25th, 2004.

Professor Werner Massa zum 60. Geburtstag gewidmet

Abstract. Reaction of the binuclear μ -carbamoyl complex $[(\text{CO})_3\text{Fe}(\mu\text{-Me}_2\text{NCO})_2\text{Fe}(\text{CO})_2(\text{HNMe}_2)]$ (**1**) in toluene with the chelating ligands $\text{Ph}_2\text{PCH}_2\text{PPh}_2$ (dppm) and $\text{Ph}_2\text{PCH}_2\text{CH}_2\text{PPh}_2$ (dppe) gives different results. With dppm only the complex $[(\text{CO})_3\text{Fe}(\mu\text{-Me}_2\text{NCO})_2\text{Fe}(\text{CO})_2(\text{dppm})]$ (**3**) with a dangling ligand is obtained under replacement of amine, whereas with dppe depending on the reaction conditions up to three compounds are found. A 1 : 1 mixture of the educts generates the related complex $[(\text{CO})_3\text{Fe}(\mu\text{-Me}_2\text{NCO})_2\text{Fe}(\text{CO})_2(\text{dppe})]$ (**4**) together with the tetranuclear complex $\{[(\text{CO})_3\text{Fe}(\mu\text{-Me}_2\text{NCO})_2\text{Fe}(\text{CO})_2]_2(\text{dppe})\}$ (**5**). **4** slowly converts into $[(\text{CO})_3\text{Fe}(\mu\text{-Me}_2\text{NCO})_2\text{Fe}(\text{CO})(\text{dppe})]$ (**6**) with

dppe acting as a chelating ligand. **6** is the first compound in this series in which one of the five CO groups is replaced by another donor. A 2 : 1 molar ratio of **1** and dppe quantitatively produces **5**. Addition of CO to a solution of **6** proceeds under slow reversible conversion of the complex into **4**. The compounds were characterized by the usual spectroscopic methods; **3**, **5**, and **6** were also studied by X-ray diffraction analyses.

Keywords: Iron; Chelating ligands; Bridging carbamoyl groups; Crystal structures

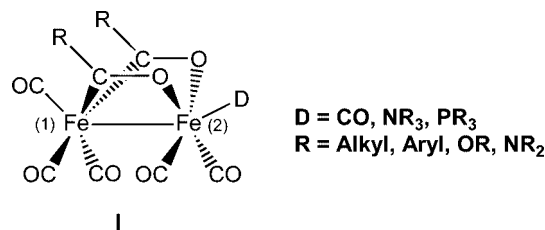
Über die Reaktion von $[(\text{CO})_3\text{Fe}(\mu\text{-Me}_2\text{NCO})_2\text{Fe}(\text{CO})_2(\text{NHMe}_2)]$ mit Chelatliganden – Kristallstrukturen neuer zweikerniger μ -Carbamoyl Komplexe

Inhaltsübersicht. Die Reaktion des zweikernigen μ -Carbamoylkomplexes $[(\text{CO})_3\text{Fe}(\mu\text{-Me}_2\text{NCO})_2\text{Fe}(\text{CO})_2(\text{HNMe}_2)]$ (**1**) mit den Chelatliganden $\text{Ph}_2\text{PCH}_2\text{PPh}_2$ (dppm) und $\text{Ph}_2\text{PCH}_2\text{CH}_2\text{PPh}_2$ (dppe) führt zu unterschiedlichen Ergebnissen. Mit dppm entsteht durch Verdrängung des Amins der Komplex $[(\text{CO})_3\text{Fe}(\mu\text{-Me}_2\text{NCO})_2\text{Fe}(\text{CO})_2(\text{dppm})]$ (**3**) mit einem frei baumelnden Liganden, wohingegen mit dppe je nach Reaktionsbedingungen bis zu drei Verbindungen gefunden werden. Eine 1 : 1 Umsetzung der Edukte liefert den zu **3** analogen Komplex $[(\text{CO})_3\text{Fe}(\mu\text{-Me}_2\text{NCO})_2\text{Fe}(\text{CO})_2(\text{dppe})]$ (**4**) zusammen mit dem vierkernigen Komplex $\{[(\text{CO})_3\text{Fe}(\mu\text{-Me}_2\text{NCO})_2\text{Fe}(\text{CO})_2]_2(\text{dppe})\}$ (**5**). Der Komplex **4** wandelt sich langsam unter CO-Verlust in $[(\text{CO})_3\text{Fe}(\mu\text{-Me}_2\text{NCO})_2\text{Fe}(\text{CO})(\text{dppe})]$ (**6**) um, wobei dppe als Chelatligand fungiert. **6** ist die erste Verbindung in dieser Serie, in der eine der fünf CO-Gruppen durch einen Fremddonor ersetzt ist. Ein 2 : 1 Molverhältnis von **1** und dppe liefert quantitativ **5**. Einleiten von CO in eine Lösung von **6** führt langsam zur reversiblen Rückverwandlung in **4**. Die Verbindungen wurden durch die üblichen spektroskopischen Methoden charakterisiert; **3**, **5** und **6** wurden auch durch Kristallstrukturanalysen bestimmt.

$[(\text{CO})_3\text{Fe}(\mu\text{-Me}_2\text{NCO})_2\text{Fe}(\text{CO})_2(\text{dppe})]$ (**5**). Der Komplex **4** wandelt sich langsam unter CO-Verlust in $[(\text{CO})_3\text{Fe}(\mu\text{-Me}_2\text{NCO})_2\text{Fe}(\text{CO})(\text{dppe})]$ (**6**) um, wobei dppe als Chelatligand fungiert. **6** ist die erste Verbindung in dieser Serie, in der eine der fünf CO-Gruppen durch einen Fremddonor ersetzt ist. Ein 2 : 1 Molverhältnis von **1** und dppe liefert quantitativ **5**. Einleiten von CO in eine Lösung von **6** führt langsam zur reversiblen Rückverwandlung in **4**. Die Verbindungen wurden durch die üblichen spektroskopischen Methoden charakterisiert; **3**, **5** und **6** wurden auch durch Kristallstrukturanalysen bestimmt.

1 Introduction

Recently, we described some new compounds which belong to a series of unique asymmetrically bridged dinuclear iron compounds of the type **I** [1]. These complexes have in common that only the ligand in the position D, which we have named the “ α ” position, has been replaced by other donor ligands. The labilized position is located trans to Fe(1) within the symmetry plane of the molecule; D stands for CO and a variety of N or P donating ligands [2]. The iron atoms in **I** are chemically different, and according to the attached oxygen atoms Fe(2) is in a higher formal oxidation state than Fe(1) [5].



Scheme 1

The main and typical route to these complexes is the oxidative coupling reaction of anionic carbamoyl, acyl, or alkoxycarbonyl compounds, $[(\text{CO})_4\text{FeC}(\text{O})\text{R}]^-$. Recently, we found that oxidation of the carbamoyl complex $[\text{C}(\text{NMe}_2)_3]^{2-}$ with Ag^+ leads to the formation of $[(\text{CO})_3\text{Fe}(\mu\text{-Me}_2\text{NCO})_2\text{Fe}(\text{CO})_2(\text{HNMe}_2)]$ (**1**) with HNMe_2 in the α position [1]. Addition of PPh_3 to **1** quantitatively

* Prof. Dr. Wolfgang Petz, Prof. Dr. Bernhard Neumüller
Fachbereich Chemie der Philipps Universität
D-35032 Marburg, Hans-Meerwein-Strasse
E-mail: petz@staff.uni-marburg.de, neumuell@chemie.uni-marburg.de

gives $[(\text{CO})_3\text{Fe}(\mu\text{-Me}_2\text{NCO})_2\text{Fe}(\text{CO})_2(\text{PPh}_3)]$ (**2**) indicating that HNMe_2 is a good leaving group. These properties prompted us to study the reactivity of **1** more intensively, and in this contribution we report on the results of the reaction of **1** with the diphosphines $\text{Ph}_2\text{PCH}_2\text{PPh}_2$ (dppm) and $\text{Ph}_2\text{PCH}_2\text{CH}_2\text{PPh}_2$ (dppe). In choosing chelating ligands, we also studied the possibility of replacing a further carbonyl group additionally to the replacement of a ligand in the α position with help of the chelating effect. To our knowledge, no bidentate ligands with N or P donating atoms have been introduced into **1** as yet and no compounds with more than one donor ligand instead of CO at any other position have been obtained. Three of the new products could be characterized by X-ray analyses.

2 Results and Discussion

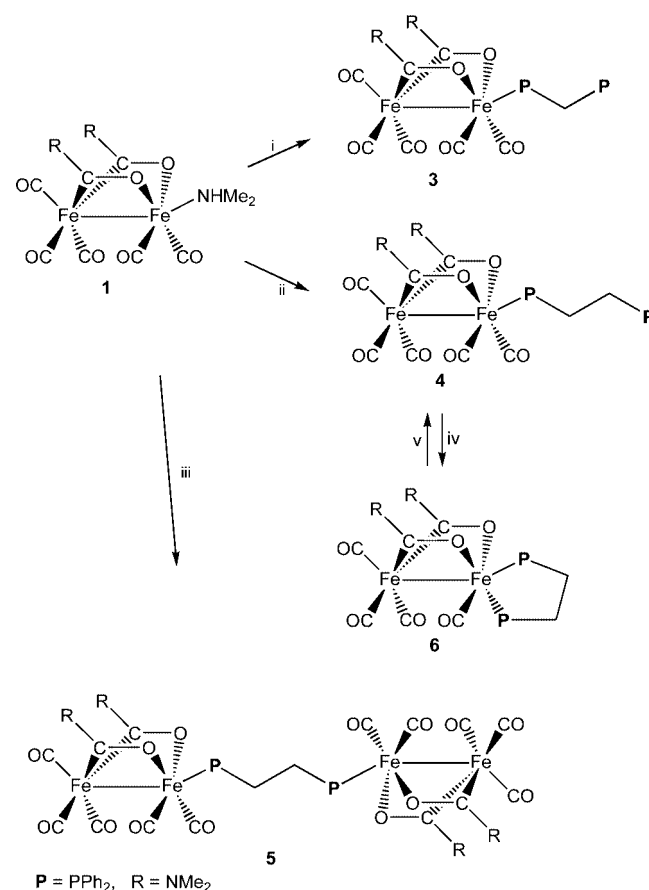
2.1 Preparation and properties

Similar to the preparation of $[(\text{CO})_3\text{Fe}(\mu\text{-Me}_2\text{NCO})_2\text{Fe}(\text{CO})_2(\text{PPh}_3)]$ (**2**) [1], complex **1** reacts with dppm under substitution of HNMe_2 to give quantitatively the complex $[(\text{CO})_3\text{Fe}(\mu\text{-Me}_2\text{NCO})_2\text{Fe}(\text{CO})_2(\eta^1\text{-PPh}_2\text{CH}_2\text{PPh}_2)]$ (**3**), in which the α position is now occupied by one phosphorus atom of the dppm ligand. The ^{31}P NMR spectrum of **3** exhibits a pair of doublets at 41.5 ppm and -27.5 ppm ($^2J(\text{P,P}) = 59.8$ Hz). The low field signal is located near the signal of **2** and the high field signal is close to that of the free ligand, indicating the presence of a dangling ligand instead of a chelating one. Heating of the reaction mixture or longer reaction time or addition of another equivalent of **1** do not alter the spectrum, which means that neither a chelating effect occurs with substitution of a further carbonyl group nor a second diiron fragment can be added to the free phosphorus atom of the dppm ligand. In contrast to our findings, the photochemical reaction of dppm with $\text{Fe}(\text{CO})_5$ generates all possible products [8], and similar pairs of doublets were observed in the complex $[\text{Fe}(\text{CO})_4(\eta^1\text{-dppm})]$, however, with a stronger low field shift of the FePPh_2 signal and larger coupling constants [7].

The results completely change if the distance between the phosphorus atoms is increased e.g. separated by a further CH_2 group as in dppe. In contrast to the dppm ligand, the results of the reaction of **1** with dppe depend on the ratio of the reactants, temperature, and reaction time. Thus, a 1:1 molar ratio of the reactants at room temperature gives a mixture of $[(\text{CO})_3\text{Fe}(\mu\text{-Me}_2\text{NCO})_2\text{Fe}(\text{CO})_2(\eta^1\text{-PPh}_2\text{CH}_2\text{CH}_2\text{PPh}_2)]$ (**4**) with a dangling ligand and the tetranuclear complex $[\{(\text{CO})_3\text{Fe}(\mu\text{-Me}_2\text{NCO})_2\text{Fe}(\text{CO})_2\}_2\text{-}(\text{dppe})]$ (**5**) in which both positions of dppe are occupied by a diiron fragment; the ratio of **4** to **5** to unreacted dppe was recorded as 2:1:1, respectively. Similar to **3** the ^{31}P NMR spectrum of **4** exhibits a pair of doublets at 41.2 ppm and -12.2 ppm ($^3J(\text{P,P}) = 36.9$ Hz) whereas for **5** a singlet at 41.7 ppm is recorded, which is due to equivalent phosphorus atoms. At a threefold excess of dppe and slow addition of **1** to the solution of dppe to avoid a local high

concentration of **1** mainly **4** is generated and the formation of **5** is nearly suppressed. However, with time a further pair of doublets at 88.3 and 65.7 ppm ($^3J(\text{P,P}) = 22.9$ Hz) appears which can be assigned to $[(\text{CO})_3\text{Fe}(\mu\text{-Me}_2\text{NCO})_2\text{Fe}(\text{CO})(\text{dppe})]$ (**6**), in which the dppe now acts as a chelating ligand under replacement of a further CO group at Fe(2). The ratio of complex **4** to complex **6** under these conditions was 1:0.3. On heating the NMR tube at about 40°C for about 30 minutes the signals of **4** decreased in favor of **6**, and a **4:6** ratio of 1:5.4 was recorded. The complex **6** is the first one, in which two positions in **1** are occupied by a non carbonyl ligand. The signals of **6** increase with time, and on standing of the reaction mixture at room temperature for several days the signals of **4** disappeared. Crystal growth from the solution needs several days and produces only red crystals of **6**. The conversion of **4** into **6** is reversible at room temperature on exposure to an atmosphere of CO (1 atm) as shown by ^{31}P NMR experiments. Thus, stirring a toluene solution of **6** under CO, the **6** to **4** ratio was recorded as 1:0.09 after 3 h and increased to 1:0.4 after 12 h of exposure to CO.

When a 1:2 ligand to iron complex **1** ratio is allowed to react, quantitatively the tetranuclear complex **5** is produced



Scheme 2 (i) 1 equiv. of dppm in toluene, (ii) excess dppe in toluene, (iii) 1/2 equivalent dppe, (iv) 1 d at room temperature, (v) 1 atm CO, 3h

as shown by ^{31}P NMR studies; the singlet at 41.7 ppm was recorded as the single absorption. Addition of further dppe to a reaction mixture with a given 4:5 ratio does not change the initial ratio in favor to **4**, which means that phosphine ligands are bonded stronger than N donating ligands and ligand exchange does not occur in this case in the α position. Thus, only amines such as HNMe_2 in the α position act as excellent leaving groups.

The difference in the reactivity of **3** and **4** towards **1** may be originated by a steric effect. The free phosphorus atom in **3** can be considered as a diphenylphosphine with a very large third substituent and with a large cone angle preventing coordination at a metal atom; in **4**, however, the second phosphorus atom is too far away and free for coordination.

The IR data of **3** and **5** in the carbonyl region are very similar to those of **2** [1]. Three or four very strong absorptions between 2030 and 1920 cm^{-1} were found for the five terminal CO groups in the metallacyclic compounds with a local C_s symmetry. The additional coordination of a phosphorus atom as in **6** causes the $\nu(\text{CO})$ bands to shift to lower frequencies according to the increased back donation of electron density into CO π^* orbitals of the remaining carbonyl groups. For the four CO groups, the loss of the molecular C_s symmetry gives rise to four strong bands at 1985, 1930, 1919, and 1887 cm^{-1} . In all compounds absorp-

tions around 1500 cm^{-1} were recorded and tentatively assigned to the bridging carbamoyl group.

The ^1H and ^{13}C NMR spectra of **6** confirm that the structure of the molecule is rigid on the NMR time scale. Both spectra exhibit four signals for the NMe_2 groups due to the lack of a molecular symmetry plane and according to restricted rotation at the C– NMe_2 bond. Compared to **3** in the ^1H NMR spectrum of **6** the low field pair at 2.86/2.28 ppm can be attributed to the NMe_2 group trans to CO, whereas the pair 2.68/2.20 ppm belongs to the carbamoyl group trans to the phosphorus atom. A similar assignment can be made for the two pairs of NMe_2 signals at 39.4/35.2 and 39.0/35.1 ppm in the ^{13}C NMR spectrum of **6**. For the four terminal CO groups and the two carbenoid carbamoyl carbon atoms six signals were expected; however, the low solubility of **6** in toluene did not allow to detect the corresponding signals.

If only the α position in the molecular symmetry plane is occupied by various donor molecules only two absorptions are found for the type **I** compounds due to the hindered rotation about the C–N bond. The entrance of the second dppe phosphorus atom into the coordination sphere of the metal atom in **6** causes a low field shift of both signals in the ^{31}P NMR spectrum; the signal at the lowest field at 88.3 ppm is assigned to the phosphorus atom trans to the carbamoyl oxygen atom.

Table 1 Crystal data and structure refinement details for **3**, **5** and **6**

	3	5	6
formula	$\text{C}_{36}\text{H}_{34}\text{Fe}_2\text{N}_2\text{O}_7\text{P}_2$	$\text{C}_{48}\text{H}_{48}\text{Fe}_4\text{N}_4\text{O}_{14}\text{P}_2$	$\text{C}_{36}\text{H}_{36}\text{Fe}_2\text{N}_2\text{O}_6\text{P}_2$
mw (g/mol)	780.31	1190.26	766.33
a/pm	1200.1(1)	1067.4(2)	1212.1(1)
b/pm	1018.7(1)	1615.9(2)	3125.4(2)
c/pm	2933.4(2)	1524.5(2)	961.0(1)
$\beta/^\circ$	96.43(1)	99.11(1)	110.58(1)
crystal size/mm	$0.43 \times 0.43 \times 0.42$	$0.15 \times 0.1 \times 0.06$	$0.31 \times 0.15 \times 0.05$
volume/ $\text{pm}^3 \cdot 10^6$	3563.6(5)	2596.3(8)	3408.2(5)
Z	4	2	4
d_{calc} (g/cm^3)	1.454	1.523	1.493
crystal system	monoclinic	monoclinic	monoclinic
space group	$\text{P}2_1/\text{c}$ (Nr. 14)	$\text{P}2_1/\text{c}$ (No. 14)	$\text{P}2_1/\text{n}$ (No. 14)
diffractometer	IPDS II (Stoe)	IPDS I (Stoe)	IPDS II (Stoe)
radiation	Mo- $\text{K}\alpha$	Mo- $\text{K}\alpha$	Mo- $\text{K}\alpha$
temperature /K	193	193	193
μ/cm^{-1}	9.5	12.2	9.9
$2\theta_{\text{max}}/^\circ$	52.58	52.36	52.39
index range	$-14 \leq h \leq 14$ $-12 \leq k \leq 12$ $-36 \leq l \leq 36$	$-13 \leq h \leq 13$ $-19 \leq k \leq 19$ $-18 \leq l \leq 18$	$-15 \leq h \leq 13$ $-38 \leq k \leq 38$ $-11 \leq l \leq 11$
number of rflns collected	49398	23051	33126
number of indep. rflns (R_{int})	7189 (0.036)	5070 (0.231)	6809 (0.0905)
number of observed rflns with $F_0 > 4\sigma(F_0)$	6198	1826	5127
parameters	447	330	438
absorption correction	numerical	numerical	numerical
structure solution	direct methods SHELXS-97 [9]	direct methods SIR-92 [10]	direct methods SHELXS-97 [9]
refinement against F^2	SHELXL-97 [11]	SHELXL-97 [11]	SHELXL-97 [11]
H atoms	a)	a)	a)
R_1	0.0323	0.0424	0.042
wR_2 (all data)	0.0912	0.0841	0.1086
max. electron density left/ $\text{e}/\text{pm}^3 \cdot 10^{-6}$	0.40	0.38	0.53

a) calculated positions with common displacement parameter

The NMR data are consistent with the solid state structure discussed below.

2.2 Crystal Structures

In order to get a deeper inside into the properties of the compounds, the structures of **3**, **5**, and **6** have been determined by single crystal X-ray diffraction measurements. Red crystals of the compounds were obtained at room temperature by layering the filtered toluene solutions with *n*-pentane. ORTEP views of the molecules are depicted in Figures 1 to 3; details of the structure determinations are collected in Table 1; bond distances and angles are summarized in the Tables 2 (compound **3**), 3 (compounds **5**), and 4 (compound **6**). Molecular structures of similar compounds with PPh₃ in the *a* position have been determined with R = mes, NPr¹₂ [2h], NMe₂ [1], and OBU^t [2g]. All compounds have in common the typical Fe₂C₂O₂ structural motif with the butterfly arrangement of the carbamoyl ligand.

2.2.1 Crystal structure of [(CO)₃Fe(μ-Me₂NCO)₂-Fe(CO)₂(PPh₂CH₂PPh₂)] (**3**)

The crystal structure of **3** is shown in Figure 1; it is closely related to that of the corresponding PPh₃ derivative **2** [1] and confirms the presence of only one coordinating P atom in the molecule. The largest differences are found in a slightly shorter Fe–Fe distance (about 1 pm) and a shorter Fe–P distance (about 3 pm) in **3**; all other parameters are equal. The position of the dangling free PPh₂ group is probably fixed by packing effects and the distance of the P(2) atom to the iron moiety is too far away for any interaction. The dihedral angle between the planes spanned by the atoms Fe(1), Fe(2), N(1), C(6), O(6) and Fe(1), Fe(2), N(2), C(7), O(7) is 86°. The P–C–P angle amounts to 113° and is about 3° larger than in [Fe₂(CO)₇(μ-dppm)] where both P atoms coordinate and bridge two Fe atoms [3]; however, if dppm acts as a chelating ligand as in [Fe(CO)₃(dppm)], the corresponding angle is strained to 91° [4].

2.2.2 Crystal structure of [(CO)₃Fe(μ-Me₂NCO)₂-Fe(CO)₂(PPh₂(CH₂)₂PPh₂)Fe(CO)₂(μ-Me₂NCO)₂-Fe(CO)₃] (**5**)

In the solid state the tetranuclear complex **5** crystallizes in the centrosymmetric form with the symmetry center in the middle of the C–C-bond of dppe; the molecular structure is depicted in Figure 2. One dimethylamino group is disordered and only one position is shown. The two planes containing the atoms Fe(1), Fe(2), O(6), C(6), N(11) and Fe(1), Fe(2), O(7), C(7), N(2) have a dihedral angle of 86°. As expected, in both iron moieties the favored α position is occupied by the phosphorus atoms. Most of the other distances and angles are identical with the parameters of the related compounds **2** and **3**.

Table 2 Selected bond distances/pm and angles/° in [(CO)₃Fe(μ-Me₂NCO)₂Fe(CO)₂(PPh₂CH₂PPh₂)] (**3**)

distances			
Fe(1)–Fe(2)	256.93(4)	Fe(1)–P(1)	227.12(5)
Fe(1)–O(6)	190.0(1)	Fe(1)–O(7)	197.7(1)
Fe(1)–C(1)	175.6(2)	Fe(1)–C(2)	176.3(2)
Fe(2)–C(3)	178.7(2)	Fe(2)–C(4)	179.4(2)
Fe(2)–C(5)	178.4(2)	Fe(2)–C(6)	199.4(2)
Fe(2)–C(7)	198.4(2)	P(1)–C(8)	183.3(2)
P(2)–C(8)	185.9(2)	O(1)–C(1)	115.5(2)
O(2)–C(2)	115.0(2)	O(3)–C(3)	114.8(3)
O(4)–C(4)	114.6(3)	O(5)–C(5)	114.5(3)
O(6)–C(6)	128.3(2)	O(7)–C(7)	128.3(2)
N(1)–C(6)	133.4(2)	N(2)–C(7)	134.5(2)
angles			
Fe(2)–Fe(1)–P(1)	157.74(2)	Fe(2)–Fe(1)–O(6)	73.23(4)
Fe(2)–Fe(1)–O(7)	72.91(4)	Fe(2)–Fe(1)–C(1)	102.27(6)
Fe(2)–Fe(1)–C(2)	96.35(6)	P(1)–Fe(1)–O(6)	92.01(4)
P(1)–Fe(1)–O(7)	89.46(4)	P(1)–Fe(1)–C(1)	94.15(6)
P(1)–Fe(1)–C(2)	97.96(6)	O(6)–Fe(1)–O(7)	84.48(6)
O(6)–Fe(1)–C(1)	90.08(7)	O(6)–Fe(1)–C(2)	169.58(7)
O(7)–Fe(1)–C(1)	173.58(7)	O(7)–Fe(1)–C(2)	92.56(7)
C(1)–Fe(1)–C(2)	92.20(9)	Fe(1)–Fe(2)–C(3)	173.38(7)
Fe(1)–Fe(2)–C(4)	89.15(7)	Fe(1)–Fe(2)–C(5)	92.82(7)
Fe(1)–Fe(2)–C(6)	68.37(5)	Fe(1)–Fe(2)–C(7)	69.15(5)
C(3)–Fe(2)–C(4)	92.4(1)	C(3)–Fe(2)–C(5)	93.45(9)
C(3)–Fe(2)–C(6)	104.80(8)	C(3)–Fe(2)–C(7)	108.92(9)
C(4)–Fe(2)–C(5)	95.0(1)	C(4)–Fe(2)–C(6)	90.65(8)
C(4)–Fe(2)–C(7)	158.20(8)	C(5)–Fe(2)–C(6)	160.66(8)
C(5)–Fe(2)–C(7)	88.33(9)	C(6)–Fe(2)–C(7)	79.85(7)
Fe(1)–P(1)–C(8)	113.10(6)	Fe(1)–P(1)–C(9)	110.05(6)
Fe(1)–P(1)–C(15)	120.54(6)	C(8)–P(1)–C(9)	104.19(8)
C(8)–P(1)–C(15)	103.21(8)	C(9)–P(1)–C(15)	104.21(8)
Fe(1)–O(7)–C(7)	105.5(1)	Fe(1)–O(6)–C(6)	105.9(1)
C(6)–N(1)–C(62)	120.2(2)	C(6)–N(1)–C(61)	124.1(2)
C(7)–N(2)–C(71)	120.8(2)	C(61)–N(1)–C(62)	115.4(2)
C(71)–N(2)–C(72)	115.6(2)	C(7)–N(2)–C(72)	123.4(2)
Fe(1)–C(2)–O(2)	178.4(2)	Fe(1)–C(1)–O(1)	176.5(2)
Fe(2)–C(4)–O(4)	177.7(2)	Fe(2)–C(3)–O(3)	170.9(2)
Fe(2)–C(6)–O(6)	112.0(1)	Fe(2)–C(5)–O(5)	178.3(2)
O(6)–C(6)–N(1)	114.9(2)	Fe(2)–C(6)–N(1)	133.1(1)
Fe(2)–C(7)–N(2)	132.0(1)	Fe(2)–C(7)–O(7)	112.5(1)
P(1)–C(8)–P(2)	112.64(9)	O(7)–C(7)–N(2)	115.5(2)

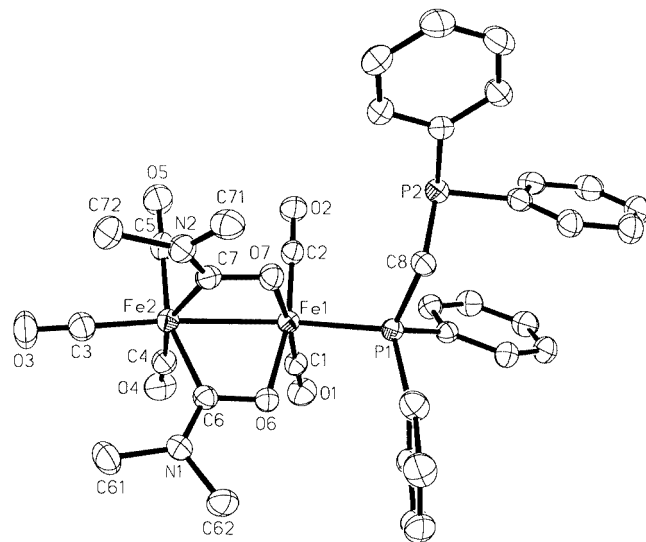
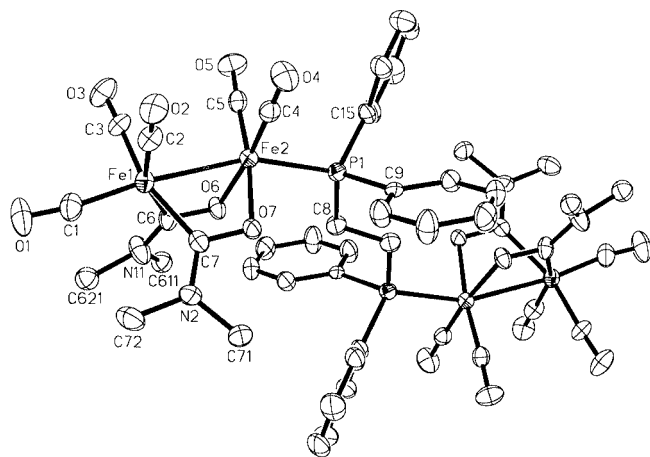


Fig. 1 Structure of **3** (40% probability for thermal ellipsoids)

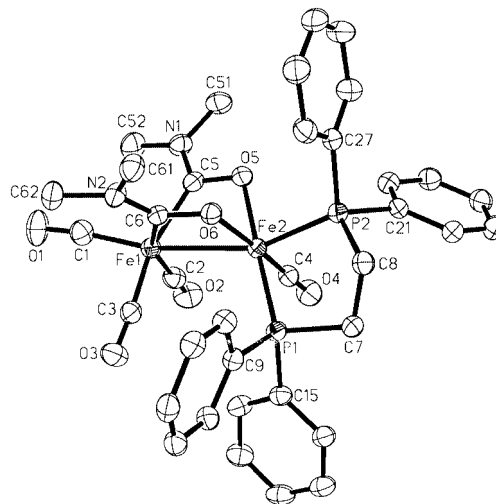
Table 3 Selected bond distances/pm and angles/ $^\circ$ in $[(\text{CO})_3\text{Fe}(\mu\text{-Me}_2\text{NCO})_2\text{Fe}(\text{CO})_2(\text{PPh}_2\text{CH}_2\text{CH}_2\text{PPh}_2)\text{Fe}(\text{CO})_2(\mu\text{-Me}_2\text{NCO})_2\text{Fe}(\text{CO})_3]$ (**5**)

distances			
Fe(1)–Fe(2)	257.9(1)	Fe(1)–C(1)	178.5(7)
Fe(1)–C(2)	179.3(7)	Fe(1)–C(3)	179.7(8)
Fe(1)–C(6)	198.0(6)	Fe(1)–C(7)	197.3(7)
Fe(2)–P(1)	228.8(2)	Fe(2)–O(6)	199.3(3)
Fe(2)–O(7)	196.9(5)	Fe(2)–C(4)	174.4(6)
Fe(2)–C(5)	175.7(8)	P(1)–C(8)	183.8(5)
O(1)–C(1)	115.7(8)	O(2)–C(2)	114.6(7)
O(3)–C(3)	112.9(9)	O(4)–C(4)	116.4(6)
O(5)–C(5)	114.2(8)	O(6)–C(6)	126.0(7)
O(7)–C(7)	127.7(7)	N(2)–C(7)	135.6(9)
N(11)–C(6)	135.0(7)	N(11)–C(611/2)	147(1)
N(11)–C(622/1)	149(1)	C(8)–C(8a)	152(1)
angles			
Fe(2)–Fe(1)–C(1)	173.2(3)	Fe(2)–Fe(1)–C(2)	90.2(2)
Fe(2)–Fe(1)–C(3)	91.1(2)	Fe(2)–Fe(1)–C(6)	68.6(2)
Fe(2)–Fe(1)–C(7)	69.0(2)	C(1)–Fe(1)–C(2)	93.8(3)
C(1)–Fe(1)–C(3)	94.0(3)	C(1)–Fe(1)–C(6)	107.1(3)
C(1)–Fe(1)–C(7)	105.4(3)	C(2)–Fe(1)–C(3)	95.7(3)
C(2)–Fe(1)–C(6)	158.7(3)	C(2)–Fe(1)–C(7)	91.1(3)
C(3)–Fe(1)–C(6)	86.7(3)	C(3)–Fe(1)–C(7)	159.0(6)
C(6)–Fe(1)–C(7)	80.0(3)	Fe(1)–Fe(2)–P(1)	159.50(7)
Fe(1)–Fe(2)–O(6)	72.5(1)	Fe(1)–Fe(2)–O(7)	72.4(1)
Fe(1)–Fe(2)–C(4)	100.5(2)	Fe(1)–Fe(2)–C(5)	101.2(2)
P(1)–Fe(2)–O(6)	93.7(1)	P(1)–Fe(2)–O(7)	91.5(1)
P(1)–Fe(2)–C(4)	93.4(2)	P(1)–Fe(2)–C(5)	94.0(2)
O(6)–Fe(2)–O(7)	84.2(2)	O(6)–Fe(2)–C(4)	172.9(2)
O(6)–Fe(2)–C(5)	90.8(2)	O(7)–Fe(2)–C(4)	95.1(3)
O(7)–Fe(2)–C(5)	172.8(2)	C(4)–Fe(2)–C(5)	89.2(3)
Fe(2)–P(1)–C(8)	110.1(2)	Fe(2)–P(1)–C(9)	117.3(2)
Fe(2)–P(1)–C(15)	115.1(2)	C(8)–P(1)–C(9)	107.0(3)
C(8)–P(1)–C(15)	105.3(3)	C(9)–P(1)–C(15)	101.0(3)
Fe(2)–O(6)–C(6)	104.9(3)	Fe(2)–O(7)–C(7)	106.0(4)
C(7)–N(2)–C(71)	119.8(5)	C(7)–N(2)–C(72)	122.7(5)
C(71)–N(2)–C(72)	116.8(6)	C(6)–N(11)–C(611)	120.6(7)
C(612)–N(11)–C(622)	120.4(8)	C(6)–N(11)–C(612)	119.1(7)
C(6)–N(11)–C(622)	120.2(7)	Fe(1)–C(1)–O(1)	171.3(7)
Fe(1)–C(2)–O(2)	179.7(7)	Fe(1)–C(3)–O(3)	176.3(6)
Fe(2)–C(4)–O(4)	177.3(6)	Fe(2)–C(5)–O(5)	177.6(5)
Fe(1)–C(6)–O(6)	114.0(4)	Fe(1)–C(6)–N(11)	130.3(5)
Fe(1)–C(6)–N(12)	130.3(5)	O(6)–C(6)–N(11)	115.8(5)
O(6)–C(6)–N(12)	115.8(5)	Fe(1)–C(7)–O(7)	112.5(5)
Fe(1)–C(7)–N(2)	132.4(4)	O(7)–C(7)–N(2)	115.0(6)
P(1)–C(8)–C(8a)	117.6(4)		

**Fig. 2** Molecular structure of **5** (50% probability for thermal ellipsoids)

2.2.3 Crystal structure of $[(\text{CO})_3\text{Fe}(\mu\text{-Me}_2\text{NCO})_2\text{Fe}(\text{CO})(\text{PPh}_2(\text{CH}_2)_2\text{PPh}_2)]$ (**6**)

The complex **6** is the first one in which two donor atoms other than CO are bonded in a type I species. In going from **5** to **6** the occupied α position is maintained, which does not allow the dppe ligand to bridge two Fe atoms but replaces a CO group at the same atom under loss of the molecular mirror plane; the molecular structure is shown in Figure 3. The coordination of the second phosphorus atom increases the Fe–Fe-bond length by about 6 pm; this is the largest iron iron bond separation found in this series of compounds. As in similar compounds, both iron atoms are approximately in an octahedral environment. The phosphorus atom opposite to the Fe–Fe bond in the α position is about three pm further away from Fe(2) than that opposite to O(5). Also the Fe–O distances are slightly different; as expected, the oxygen atom trans to CO is closer to Fe(2) than that trans to P(1). The replacement of one of the two carbonyl groups at Fe(2) by a better σ -donor increases $d\text{-}\pi^*$ back donation to the remaining CO group with the effect of a shortening of the carbon-iron bond distance to about 174 pm. The lack of a symmetry plane induces chirality at Fe(2) and the unit cell contains the pair of enantiomers. The corresponding dihedral angle between the two Fe_2CON planes amounts to 83.2° .

**Fig. 3** Molecular structure of **6** (50% probability for thermal ellipsoids)

2.2.4 Conclusion and outlook

In the unique binuclear iron complexes **I** as yet only the α position has been replaced by other donating ligands and the five remaining carbonyl groups are very strongly bonded. However, it is possible to attack a further CO position with the chelating ligands dppe, but at first the easier attainable α position is occupied serving as an anchoring position for the chelating ligand. Thus, **6** represents the first complex in this series containing four CO and two other donor ligands. Starting with one donor atom in the α position

Table 4 Selected bond distances/pm and angles/° in [(CO)₃Fe(μ-Me₂NCO)₂Fe(CO)(PPh₂CH₂CH₂PPh₂)] (**6**)

distances			
Fe(1)–Fe(2)	263.15(5)	Fe(1)–C(1)	178.6(3)
Fe(1)–C(2)	177.9(3)	Fe(1)–C(3)	177.3(3)
Fe(1)–C(5)	199.8(3)	Fe(1)–C(6)	200.4(3)
Fe(2)–P(1)	221.17(8)	Fe(2)–P(2)	224.42(8)
Fe(2)–O(5)	198.4(2)	Fe(2)–O(6)	196.7(2)
Fe(2)–C(4)	174.0(3)	P(1)–C(7)	186.9(3)
P(1)–C(9)	183.5(3)	P(1)–C(15)	183.1(3)
P(2)–C(8)	183.3(3)	P(2)–C(21)	182.1(3)
P(2)–C(27)	182.8(3)	O(1)–C(1)	115.6(4)
O(2)–C(2)	115.4(4)	O(3)–C(3)	116.2(4)
O(4)–C(4)	116.3(4)	O(5)–C(5)	126.9(3)
O(6)–C(6)	127.7(3)	N(1)–C(5)	135.7(4)
N(2)–C(6)	134.9(4)	C(7)–C(8)	153.1(4)
angles			
Fe(2)–Fe(1)–C(1)	167.4(1)	Fe(2)–Fe(1)–C(2)	88.9(1)
Fe(2)–Fe(1)–C(3)	95.4(1)	Fe(2)–Fe(1)–C(5)	67.27(7)
Fe(2)–Fe(1)–C(6)	67.17(7)	C(1)–Fe(1)–C(2)	98.7(2)
C(1)–Fe(1)–C(3)	93.6(2)	C(1)–Fe(1)–C(5)	103.2(1)
C(1)–Fe(1)–C(6)	105.0(1)	C(2)–Fe(1)–C(3)	97.2(2)
C(2)–Fe(1)–C(5)	85.5(2)	C(2)–Fe(1)–C(6)	156.1(1)
C(3)–Fe(1)–C(5)	162.5(1)	C(3)–Fe(1)–C(6)	85.1(1)
C(2)–Fe(1)–C(3)	85.6(1)	Fe(1)–Fe(2)–P(1)	108.76(3)
Fe(1)–Fe(2)–P(2)	156.38(3)	Fe(1)–Fe(2)–O(5)	72.37(6)
Fe(1)–Fe(2)–O(6)	72.90(6)	Fe(1)–Fe(2)–C(4)	101.4(1)
P(1)–Fe(2)–P(2)	86.95(3)	P(1)–Fe(2)–O(5)	178.85(7)
P(1)–Fe(2)–O(6)	95.10(6)	P(1)–Fe(2)–C(4)	87.8(1)
P(2)–Fe(2)–O(5)	91.72(6)	P(2)–Fe(2)–O(6)	88.60(6)
P(2)–Fe(2)–C(4)	96.6(1)	O(5)–Fe(2)–O(6)	84.39(8)
O(5)–Fe(2)–C(4)	92.9(1)	O(6)–Fe(2)–C(4)	174.2(1)
Fe(2)–P(1)–C(7)	107.35(9)	Fe(2)–P(1)–C(9)	121.79(9)
Fe(2)–P(1)–C(15)	120.09(9)	C(7)–P(1)–C(9)	101.3(1)
C(7)–P(1)–C(15)	102.1(1)	C(9)–P(1)–C(15)	101.2(1)
Fe(2)–P(2)–C(8)	107.98(9)	Fe(2)–P(2)–C(21)	116.54(9)
Fe(2)–P(2)–C(27)	115.59(9)	C(8)–P(2)–C(21)	105.1(1)
C(8)–P(2)–C(27)	105.4(1)	C(21)–P(2)–C(27)	105.2(1)
Fe(2)–O(5)–C(5)	105.0(2)	Fe(2)–O(6)–C(6)	105.6(2)
C(5)–N(1)–C(51)	120.1(3)	C(5)–N(1)–C(52)	125.0(3)
C(51)–N(1)–C(52)	114.8(3)	C(6)–N(2)–C(61)	120.1(2)
C(6)–N(2)–C(62)	123.4(3)	C(61)–N(2)–C(62)	116.6(3)
Fe(1)–C(1)–O(1)	173.4(4)	Fe(1)–C(2)–O(2)	178.5(3)
Fe(1)–C(3)–O(3)	176.2(3)	Fe(2)–C(4)–O(4)	178.6(3)
Fe(1)–C(5)–O(5)	114.4(2)	Fe(1)–C(5)–N(1)	130.9(2)
O(5)–C(5)–N(1)	114.6(2)	Fe(1)–C(6)–O(6)	114.3(2)
Fe(1)–C(6)–N(2)	130.7(2)	O(6)–C(6)–N(2)	115.0(2)

as in **3** and **4**, in no case a symmetric arrangement of the chelating ligand would be possible. Further, a rearrangement in which the two CO groups out of the symmetry plane of the diiron fragment either at Fe(1) or Fe(2) are replaced, is not observed, too.

With **I** high nuclear dendrimers may be available with suitable branched phosphines as well as compounds of the type [L_nM(PPh₂(CH₂)_xPPh₂)_xM'L_n] with different transition metal fragments at both ends of the chelating ligand if a freshly prepared complex **4** or a similar species [(CO)₃Fe(μ-Me₂NCO)₂Fe(CO)₂(PPh₂(CH₂)_xPPh₂)] (x > 1) is treated with a 16 electron fragment. However, the question is open, whether smaller 16 electron fragments than the dinuclear iron species may be able to occupy the free P position of **3** with x = 1. Additionally, compounds of the type **I** with a good leaving group may be interesting for catalytic purposes. Further studies in this area are in progress.

3 Experimental Section

All operations were carried out under an argon atmosphere in dried and degassed solvents using Schlenk techniques. The solvents were thoroughly dried and freshly distilled prior to use. The IR spectra were run on a Nicolet 510 spectrometer. For the NMR spectra we used the instruments Bruker AMX 500 and AC 200. Elemental analyses were performed by the analytical service of the Fachbereich Chemie der Universität Marburg (Germany). **1** was prepared according to the literature procedure [1] from [C(NMe₂)₃][(CO)₄-FeC(O)NMe₂] [6] with Ag⁺. Commercial available dpmm and dppe were used without further purification.

[(CO)₃Fe(μ-Me₂NCO)₂Fe(CO)₂(dpmm)] (**3**): To a solution of 0.44 g (0.55 mmol) of **1** in about 10 mL of toluene 0.22 g (0.55 mmol) of Ph₂PCH₂PPh₂ (dpmm) was added at room temperature and the mixture stirred for 12 h. The mixture was filtered and the clear red solution layered with pentane. After standing for a week, few small dark red crystals separated. The solution was decanted from the crystals. Concentration of the solution to half of its volume and addition of pentane gave an orange red powder, which was filtered and dried in vacuum. Yield about 0.30 g (0.39 mol) 70%. IR (Nujol): 2025 vs, 1964 vs, 1962 s, 1944 w (sh), 1923 vs ν(CO) cm⁻¹. ³¹P NMR (toluene): 41.5 (d, FePPh₂, ²J(P,P) = 59.8 Hz), -27.4 (d, PPh₂, ²J(P,P) = 59.8 Hz) ppm. Analyses: C 54.93 (calcd. 55.41), H 4.09 (4.39), N 3.61 (3.59) %.

[(CO)₃Fe(μ-Me₂NCO)₂Fe(CO)₂]₂(dppe)] (**5**): 0.047 g (0.11 mmol) of **1** and 0.019 g (0.047 mmol) of dppe were placed in an NMR tube and dissolved in 1 mL of toluene. After agitation in an ultrasonic bath (1500 W) for several minutes the ³¹P NMR spectrum showed only a singlet at 47.8 ppm. The solution was allowed to stand at room temperature for several weeks. During this time dark red crystals separated, which were collected; yield 90%. IR (Nujol): 2028 vs, 1981 vs, 1925 vs ν(CO). Analyses: C 47.61 (calcd. 48.43), H 4.00 (4.06), N 4.36 (4.71) %.

[(CO)₃Fe(μ-Me₂NCO)₂Fe(CO)(dppe)] (**6**): To a solution of a three-fold excess of dppe 0.411 g (1.02 mmol) in toluene a solution of 0.150 g (0.34 mmol) of **1** was added dropwise at room temperature within two hours and the mixture stirred for 20 min. The ³¹P NMR spectrum showed the formation of **4** and only small amounts of **6** along with the signal of unreacted ligand. The clear red solution was filtered, layered with pentane, and allowed to stand at room temperature. Red crystals of **6** separated after about two weeks, which were collected and dried in vacuum. **6** is less soluble in toluene than **2**, **3**, and **5**. IR (Nujol): 1985 vs, 1930 vs, 1919 vs, 1887 s ν(CO). ¹H NMR (toluene-d₈): 7.99 to 7.65 (m, Ph), 2.86, 2.68, 2.28, 2.20 (s's, MeN) ppm; (CDCl₃): 3.10, 2.91, 2.72, 2.49 (s's, MeN) ppm. ¹³C NMR (toluene-d₈): 39.4, 39.0, 35.2, 35.1 (s's, MeN) ppm. ³¹P NMR (toluene-d₈): 88.3 (d, FePPh₂, ³J(P,P) = 22.9 Hz), 65.7 (d, FePPh₂, ³J(P,P) = 22.9 Hz) ppm; (CDCl₃): 87.1 (d, FePPh₂, ³J(P,P) = 21.6 Hz), 65.6 (d, FePPh₂, ³J(P,P) = 21.6 Hz) ppm. Analyses: C 56.09 (calcd. 56.42), H 4.56 (4.74), N 3.58 (3.66) %.

Reaction of 6 with CO: CO gas was bubbled through a solution **6** in toluene of at room temperature. After three hours the ratio of **6**:**4** was recorded as 1:0.09 and increased to 1:0.4 after 12 hours as shown by ³¹P NMR experiments.

Crystallographic data for the structures have been deposited with the Cambridge Crystallographic Data Center, 12 Union Road, Cambridge CB21EZ. Copies of the data can be obtained on quoting the depository numbers CCDC 232581 (**3**), CCDC 232582 (**5**), and CCDC 232583 (**6**), (Fax: (+44)1223-336-033; E-mail: deposit@ccdc.cam.ac.uk).

We thank the Deutsche Forschungsgemeinschaft for financial support. W. P. is also grateful to the Max-Planck-Society, Munich, Germany, for financial support.

References

- [1] W. Petz, B. Neumüller, M. Esser, *Z. Anorg. Allg. Chem.* **2003**, 679, 1501.
- [2] a) *Gmelin Handbuch der Anorganischen Chemie*; Springer-Verlag: Berlin, Heidelberg, New York, **1979**; Eisen-Organische Verbindungen C1. b) E. O. Fischer, V. Kiener, D. St. P. Bunbury, E. Frank, P. F. Lidley, O. S. Mills, *J. Chem. Soc. Chem. Commun.* **1968**, 1378. c) E. O. Fischer, V. Kiener, *J. Organomet. Chem.* **1970**, 23, 215. d) E. O. Fischer, V. Kiener, *J. Organomet. Chem.* **1971**, 27, C 56. e) P. F. Lidley, O. S. Mills, *J. Chem. Soc. A* **1969**, 1279. f) B. Neumüller, W. Petz, *Organometallics* **2001**, 20, 163. g) D. Luart, N. N. le Gall, J.-Y. Salaün, L. Toupet, H. des Abbayes, *Inorg. Chim. Acta* **1999**, 291, 166. h) S. Anderson, A. F. Hill, A. M. Z. Slawin, A. P. J. White, D. J. Williams, *Inorg. Chem.* **1998**, 37, 594. i) G. Sundanarajan, J. San Fillipo Jr., *Organometallics* **1985**, 4, 606.
- [3] F. A. Cotton, J. M. Troup, *J. Am. Chem. Soc.* **1974**, 96, 4422.
- [4] F. A. Cotton, K. I. Hardcastle, G. A. Rusholme, *J. Coord. Chem.* **1973**, 2, 217.
- [5] E. Frank, D. S. P. Bunbury, *J. Chem. Soc. A* **1970**, 2143.
- [6] a) W. Petz, D. Bläser, R. Boese, *Z. Naturforsch.* **1988**, 43b, 945. b) W. Petz, *J. Organomet. Chem.* **1975**, 90, 223.
- [7] R. L. Keiter, A. R. Rheingold, J. J. Hamerski, C. K. Castle, *Organometallics* **1983**, 2, 1635.
- [8] P. A. Wegner, L. F. Evans, J. Haddock, *Inorg. Chem.* **1975**, 14, 192.
- [9] G. M. Sheldrick, SHELXS-97, Göttingen 1997.
- [10] A. Altomare, G. Cascarano, C. Giacovazzo, A. Guagliardi, M. C. Burla, G. Polidori, M. Camalli, SIR-92, Bari, Perugia, 1992.
- [11] G. M. Sheldrick, SHELXL-97, Göttingen 1997.